



HAL
open science

Disentangling Cro-Magnon: A multiproxy approach to reassociate lower limb skeletal remains and to determine the biological profiles of the adult individuals

Adrien Thibeault, Sébastien Villotte

► To cite this version:

Adrien Thibeault, Sébastien Villotte. Disentangling Cro-Magnon: A multiproxy approach to reassociate lower limb skeletal remains and to determine the biological profiles of the adult individuals. *Journal of Archaeological Science: Reports*, 2018, 21, pp.76-86. 10.1016/j.jasrep.2018.06.038 . hal-02266523

HAL Id: hal-02266523

<https://hal.science/hal-02266523>

Submitted on 19 Feb 2021

HAL is a multi-disciplinary open access archive for the deposit and dissemination of scientific research documents, whether they are published or not. The documents may come from teaching and research institutions in France or abroad, or from public or private research centers.

L'archive ouverte pluridisciplinaire **HAL**, est destinée au dépôt et à la diffusion de documents scientifiques de niveau recherche, publiés ou non, émanant des établissements d'enseignement et de recherche français ou étrangers, des laboratoires publics ou privés.

1 **Title:** Disentangling Cro-Magnon: a multiproxy approach to reassociate lower limb skeletal remains
2 and to determine the biological profiles of the adult individuals.

3 **Authors:** Adrien Thibeault¹, Sébastien Villotte²

4 **Affiliations:** 1: PACEA, University of Bordeaux. 2: PACEA, CNRS

5 **Corresponding author:**

6 Sébastien Villotte. sebastien.villotte@u-bordeaux.fr. 0033 (0)5 40 00 25 54. UMR5199 PACEA,
7 Université de Bordeaux - CNRS. Batiment B8, Allée Geoffroy Saint Hilaire, CS 50023. France - 33615
8 PESSAC CEDEX

9 **Key-words:** Gravettian; virtual anthropology; articulating bone portions; pair matching; cortical
10 thickness.

11 **Abstract:** Cro-Magnon is one of the most famous archeological sites in the World, but few scholars
12 are aware that the human remains from this shelter have been commingled since 1868 and that only
13 one comprehensive attempt to reassociate the bones has been published, more than fifty years ago.
14 The aim of this article is to present the results of a multiproxy approach applied in order to
15 reassociate the main bones of the lower limbs (including the pelvis) of the adults from Cro-Magnon.
16 We used a classical approach (i.e. the study of size, morphology, and surface alterations of the
17 bones), combined with tools from virtual anthropology, namely maximum length estimations, virtual
18 test of morphometrical similarities between possible pairs, virtual test of articular congruence, and
19 visual comparisons of cortical thickness of long bones. From the 26 bones from the lower limb under
20 study, 25 were associated with three individuals, named here Alpha (i.e. Cro-Magnon 1, an old man),
21 Beta (an old woman), and Gamma (an old man). This study increases the number of bones attributed
22 to Alpha and Beta and significantly changes the bone assemblage for the third adult.

23 **Highlights:**

24 - Cro-Magnon is one of the most famous archeological sites in the World

25 - The human remains from Cro-Magnon are commingled

26 - Classical and virtual methods are used to reassociate lower limb skeletal remains

27 - Three adults are identified from the lower limb skeletal remains

28 - This study significantly increases and changes the bone assemblage for these individuals

1 **1. Introduction**

2 At the end March 1868, human remains morphologically similar to recent humans were discovered
3 by workers at Cro-Magnon (Lartet, 1868). Their association with prehistoric artifacts and extinct
4 fauna in the same archeological layer indicated the great age of these fossils, and had quickly a
5 considerable impact (Henry-Gambier, et al., 2013a). These fossils were thus considered as
6 representative of the oldest European *Homo sapiens*, making Cro-Magnon one of the most famous
7 archeological sites in the World.

8 This discovery quickly led to excavations in or around the shelter and, in less than 50 years, it was
9 emptied (Henry-Gambier, et al., 2013a). However these "excavations" did not produced any useful
10 documentation on the stratigraphy of the site, and the main data were those provided by Lartet in
11 1868 (Henry-Gambier, et al., 2013a). Artifacts associated with the Aurignacian, the Gravettian and
12 the Solutrean cultures were identified at Cro-Magnon (Henry-Gambier, et al., 2013a). The human
13 remains were for long time considered as dating from the Early Aurignacian but it has been
14 demonstrated that they are most likely associated with the Early phase of the Gravettian (33 - 31000
15 Cal. BP) (Henry-Gambier, 2002, Henry-Gambier, et al., 2013a)¹.

16 Despite the iconic face of the "Veillard" (i.e. the "old man", Cro-Magnon 1) known globally, the fact
17 that there was no precise map of the exact locations of each skeletal element drawn at the time of
18 the discovery, and as a consequence the remains have been commingled since 1868, is not familiar
19 to the general public, nor to the scientific community. Since their discovery, the fossils have been the
20 subject of many analyses, but few scholars (e.g. Broca, 1868, Pruner-Bey, 1865-1875, Vallois and
21 Billy, 1965, Villotte, 2009) actually attempted to identify individuals beyond those defined solely from
22 the cranial remains. To date, only one comprehensive attempt to reassociate the bones has been
23 published, more than fifty years ago (Vallois and Billy, 1965).

24 The commingled nature of the Cro-Magnon human remains brings two other issues. The first one is
25 the estimation of the minimum number of individuals "buried" (see Henry-Gambier, et al. (2013a,
26 2013b) for an explanation of why the term "buried" is at least partially incorrect). Three adults are
27 mainly "identified" (the "old man": Cro-Magnon 1, the "woman": Cro-Magnon 2, another male: Cro-
28 Magnon 3), but four were distinguished based on the cranial elements soon after the discovery
29 (Broca, 1868, Lartet, 1868). According to Vallois and Billy (1965), Cro-Magnon 4 (the fourth
30 individual) is represented by only one cranial fragment. Immature remains were also identified at
31 Cro-Magnon, most of the authors considering that they belong to one neonate (Broca, 1868, Henry-
32 Gambier, 2008a, 2008b, Henry-Gambier, et al., 2013a, Lartet, 1868, Pruner-Bey, 1865-1875, Vallois
33 and Billy, 1965, and contra Gambier, 1986). The second issue relates to the sex and age-at-death

1 assessment of the adults. As the adults are identified (and thus named) from the cranial remains,
2 these assessments are established on the skull, whereas it has been shown that they are far less
3 reliable than those done from coxal bones, especially in prehistoric samples (Brůžek, et al., 2005,
4 Brůžek, et al., 2004). A comprehensive study on the pelvic remains of Cro-Magnon was carried out by
5 Gambier et al. (2006). They identified four adults: two males (one being old and the other likely to
6 be), one very old female, and one unsexed individual and with unknown age-at-death (Gambier, et
7 al., 2006). However, these authors did not attempt to associate non-pelvic remains to these
8 individuals.

9 The aim of the present paper is to use a multiproxy approach to attempt to reassociate the main
10 bones of the lower limbs (including the pelvis) of the adults from Cro-Magnon. The choice of focusing
11 on the lower limbs was dictated by four main reasons. First, at Cro-Magnon, the lower limb remains
12 are relatively well preserved. Second, bilateral asymmetry being often negligible for the lower limb
13 (Auerbach and Ruff, 2006), the re-association by pair is much more reliable than for upper limb
14 elements for which bilateral asymmetry can be extremely marked in Upper Paleolithic individuals
15 (e.g. Sparacello, et al., 2017). Third, by doing so, we can securely identify several sets of skeletal
16 elements associated with the pelvic remains (for which sex and age-at-death has been reliably
17 assessed) and avoid the issue of uneasy associations with cranial remains (for which age-at-death
18 determination and sex assessment may be doubtful). Finally, osteometric data from skeletal
19 elements of the lower limbs are the best ones to estimate several other core parameters of the
20 biological profile of these individuals, notably their stature, body mass, and skeletal robusticity.

21

22 **2. Material and methods**

23 *2.1. Material under study*

24 Human remains from Cro-Magnon are curated at the Musée de l'Homme (Muséum national
25 d'Histoire naturelle, Paris). A comprehensive database of the human remains from Cro-Magnon was
26 created by D. Henry-Gambier, and then completed by the second author, in collaboration with the
27 curators of the collection. This database currently has 139 entries, the vast majority of them
28 corresponding to only one bone or bone fragment. Each entry is labeled by a unique identifying code,
29 based on the original code of the Musée de l'Homme when possible, or newly created (in case of
30 duplicates). 40 entries² refer to adult skeletal elements from the lower limbs (including the pelvic
31 girdle) (Table 1). The pedal remains, excepting the two tali and one calcaneus, were not included in
32 the present analysis. This study thus focuses on 26 bones (see supplementary material 1 for a picture

1 of each bone). Microtomodensitometric data of these bones were acquired in 2017 at the AST-RX
 2 platform in the Natural Museum of Natural History, Paris. They were obtained with the microfocus
 3 tube of the micro-CT scanner “v|tome|xL 240” (GE Sensing and Inspection Technologies Phoenix X
 4 ray). Each final volume was then reconstructed with an isotropic voxels ranging from 89 to 144 µm
 5 and using the software NRecon v2.0 (Bruker microCT) in 16-bit format.

SV code	MNHN code	Bone	Preservation
4316b	4316	Right coxal	Fragment of iliac crest
4316a	4316	Right coxal	Posterior ilium
4317	4317	Right coxal	Acetabulum and ischial tuberosity
4318	4318	Right coxal	Acetabulum and ischial tuberosity
4314a	4314	Right coxal	The ischium, inferior branch of the pubis and anterior part of the ilium missing
4315	4315	Left coxal	Posterior ilium and ischium
4314b	4314	Left coxal	Posteroinferior ilium and ischium
4319	4319	Sacrum	Right auricular surface
4314c	4314	Sacrum	Three upper sacral vertebrae and the auricular surfaces
4321	4321	Right femur	Head and neck
4323	4323	Right femur	Proximal quarter of the diaphysis
4328	4328	Right femur	Distal extremity
4323 /4327	4327	Right femur	Diaphysis
4324	4324	Left femur	Proximal two-third of the diaphysis
4325	4325	Left femur	Diaphysis
4329	4329	Left femur	Distal extremity
4322	4322	Left femur	Diaphysis and fragment of neck and head
4333	4333	Right tibia	distal half of the bone
4332	4332	Right tibia	Diaphysis
4331	4331	Left tibia	distal half of the bone
4330	4330	Left tibia	Sub complete
4335	4335	Right fibula	Proximal half of the dipahysis
4334	4334	Right fibula	Sub complete
4338	4338	Right talus	Complete
4337	4337	Left talus	Complete
4336	4336	Right calcaneus	Complete
4341	4341	Left cuboïd	Complete
4339	4339	Right navicular	Complete
4340	4340	Right navicular	Complete
4342	4342	Left medial cuneiform	Complete
4344	4344	Left intermediate cuneiform	Complete
4343	4343	Left lateral cuneiform	Complete
4345 bis	4345-bis	Right metatarsal I	Complete
4345	4345	Left metatarsal I	Complete
4346	4346	Right metatarsal II	Complete

4347	4347	Right metatarsal IV	Complete
4348	4348	Left metatarsal IV	Complete
4349	4349	Right metatarsal V	Complete
4350	4350	Left metatarsal V	Proximal half of the bone
4351	4351	Left proximal phalanx I	Complete

1 Table 1. Adult skeletal elements from the lower limbs at Cro-Magnon. In bold: bones included in the
2 present study.

3

4 *2.2. Methods*

5 The objective of the present study is to identify what was called by Duday (1987) "liaisons
6 ostéologiques de second ordre", i.e. to look in the laboratory for bone associations not recorded in
7 the field. Classically, these associations are of two kinds: looking for bilateral pairs of bones or for
8 articular congruence between two or three bones. This was done in the past on Cro-Magnon remains
9 by several scholars, including the second author of the present article. This macroscopic approach led
10 to uncertain results for Cro-Magnon remains, because all articular surfaces of a given joint are not
11 always present for a given side. This conventional approach (macroscopic examinations, done by the
12 second author) was thus completed with new techniques based on 3D models (applied by the first
13 author). The multiproxy approach used in the present study was chosen to take advantage of the
14 strength of both classical and virtual approaches. The classical approach allows identifying subtle
15 morphological characteristics, as multiple foramina, venous imprints and other small anatomical
16 features, whereas 3D models are extremely helpful for virtual test of articular congruence and virtual
17 test of similarities between possible pairs. All of these approaches, described in details in the
18 following subsections, are subjective. However, it was believed that the multiplication of approaches,
19 independently applied, was the main way to get around this limitation. The real bones were never
20 seen by the first author, who analyzed the 3D models without a priori knowledge of previously
21 published associations nor receiving specific comments on possible associations from the second
22 author. All the data recorded were then synthesized by the two authors to establish a list of
23 associations ordered and defined as follow.

24 - Impossible: overlap between preserved zones of bones from the same side, or impossible articular
25 congruence.

26 - Very unlikely: attempts at association show very different morphologies or very doubtful articular
27 congruence.

28 - Possible: no overlap but no strong arguments for an association.

1 - Probable: some strong arguments for an association.

2 - Almost certain: multiple and strong arguments for an association.

3 2.2.1. Classical approach

4 The bones were analyzed by the second author several times since 2006 at the Musée de l'Homme.
5 Classical anthropological identification of each fragment was carried out. Faunal remains previously
6 identified as human sacral elements were excluded. The zonation method (Knüsel and Outram, 2004)
7 was used to look for overlapping in the preserved zones of fragments, and thus exclude the
8 association of two bones from the same side. Gross morphology, as well as specific features (e.g. bone
9 changes at attachment sites (entheses), number and location of vascular foramina, etc.) were
10 recorded. Pathological alterations were recorded as well and similar lesion expression on two or
11 more bones was noted. Osteometric and non-metric data were collected following the Martin
12 system (Bräuer, 1988) and Finnegan (1978), completed by measurements defined in Sládek et al.
13 (2000) and Murail et al. (2005). Articular congruence was checked when possible. Notes on the colors
14 of the bones, as well as presence of concretions on the surfaces, were taken.

15 2.2.2. Estimation of the femoral head size and acetabular congruence

16 In *Homo sapiens*, femoral head diameter (FHD) is very tightly correlated with acetabular diameter
17 (AD). Plavcan, et al. (2014) provided the following least squares regression based on 91 individuals:
18 $\ln(\text{FHD}) = -0.090 + 0.991 \cdot \ln(\text{AD})$, $r = 0.967$. In order to estimate AD on Cro-Magnon coxal remains (the
19 acetabulum being sometimes damaged), TIVMI (Treatment and Increased Vision for Medical
20 Imaging) software was used on surfaces rendering (STL format, obtained with Avizo v.9 (Visualization
21 Sciences Group Inc.)) of these bones. On TIVMI, fifty equidistant points were positioned along the
22 preserved acetabular margin. Then, a medium plan was extracted from all these points, which were
23 projected on this new plan (Fig. 1). The plugin "estimate circle from path 3D" was used in order to
24 create the circle that best fits this set of points. Finally, the radius of this circle was computed and
25 multiplied by two to obtain AD. A similar protocol was used to estimate the FHD of the partial heads
26 of femora 4322 and 4321 (Table 2).

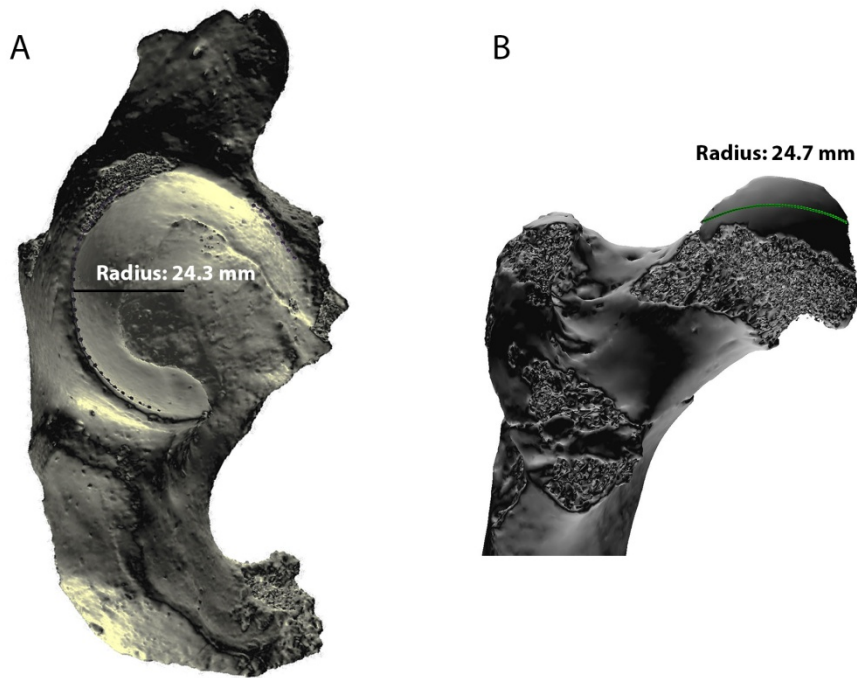
Coxal bones	Side	AD	Estimated FHD
4314a	Right	52.9	46.7
4314b	Left	55.1	48.6
4317	Right	48.6	42.9
4318	Right	56.5	49.8
4315	Left	56.7	50.0

Femora	Side	FHD	Estimated AD
4321	Right	42.2	47.8
4322	Left	49.4	56.0

1 Table 2. Computed acetabular diameters (AD) from coxal bones and head diameters (FHD) from
 2 femora, and respective estimated FHD and AD. Measurements are in millimeters.

3

4



5

6 Figure 1. Estimations of the acetabular diameter for the right coxal bone 4317 (A), and of the head
 7 diameter for the left femur 4322 (B), using TIVMI. The fifty equidistant points are projected on a
 8 medium plan. A radius is then computed for the circle that best fits this set of points.

9

10 2.2.3. Estimation of bone maximal dimensions from virtual models

11 Most of the Cro-Magnon long bones are fragmentary, with few preserved landmarks used to
 12 estimate the length of fragmentary material from regression equations (e.g. Wright and Vásquez,
 13 2003). In order to estimate the maximum length of femora, tibiae and fibulae, a well preserved set of
 14 bones from the Upper Paleolithic was used (see Table 1 in supplementary material 2). The maximum
 15 length of these bones was calculated with Netfabb Standard 2017 (Autodesk, Inc.). A surface
 16 rendering of each Cro-Magnon long bone (cf. 2.2.2) was scaled to bones of five Upper Paleolithic
 17 individuals using Meshmixer 3.4 software (Autodesk, Inc.). The product of the maximum length of the

1 bone of reference and the scaling provided an estimated maximum length. For each bone from Cro-
 2 Magnon, estimations from the five bones of reference were then averaged. An average maximum
 3 length was considered as reliable when the computed coefficient of variation (the ratio of the
 4 standard deviation to the mean) was below 2%. The results are presented in the Table 3.

SV Code	Bone	Average estimated maximum length	Standard deviation	Coefficient of variation	Minimal estimation	Maximal estimation
4328	R. Femur	475.5	7.5	1.6%	466.6	484.0
4322	L. Femur	477.0	3.6	0.8%	471.8	481.3
4323 / 4327	R. Femur	488.6	4.1	0.8%	484.4	495.1
4325	L. Femur	492.4	2.5	0.5%	488.8	494.6
4324 + 4329	L. Femur	457.5	3.0	0.7%	452.7	460.7
4330	L. Tibia	382.0	1.7	0.4%	379.2	383.4
4332	R. Tibia	394.2	5.2	1.3%	388.5	399.4
4334	R. Fibula	375.3	0.7	0.2%	374.3	375.9

5

6 Table 3. Estimations of maximum length of the long bones of the lower limb. Measurements are in
 7 millimeters.

8

9 2.2.4. Virtual test of articular congruence

10 Classically, articular congruence can be tested only for bones from the same side. We thus used
 11 surface rendering models (cf. 2.2.2) to mirror some of Cro-Magnon bones to evaluate the articular
 12 congruence of bones from different sides. In order to do so, we used surface renderings of these
 13 remains with two software programs: Meshmixer 3.4 software (Autodesk, Inc.) and MeshLab (open
 14 source).

15 2.2.5. Virtual test of morphometrical similarities between possible pairs

16 We used the same approach as in 2.2.4 in order to superimpose virtually the surface renderings of all
 17 left and right coxal bones, left and right femora, and left and right tibiae, to identify probable or
 18 improbable pairs. The distance between the two clouds of points in the overlapping area was then
 19 computed with CloudCompare 2.9.1 software (open source). One cloud is defined as the “compared
 20 cloud”, while the other one is defined as the “reference cloud”. Then, distances between the two
 21 clouds are computed: for each point of the compared cloud, CloudCompare searches the nearest

1 point in the reference cloud and computes their Euclidean distance. Finally, the reference cloud is
2 hidden and the compared cloud is colored with those distances.

3 2.2.6. Visual comparisons of cortical thickness of long bones

4 A semi-automatic threshold-based segmentation on femoral and tibial shaft with manual corrections
5 has been carried out following the Half-Maximum Height method (Spoor, et al., 1993) and by taking
6 repeated measurements on 10 random slices of the virtual stack (Coleman and Colbert, 2007) using
7 Avizo v.9 (Visualization Sciences Group Inc.) and Fiji v.1.51s (Schindelin, et al., 2012). Due to
8 preservation, the segmentation of femoral and tibial shafts has undefined boundaries. Then,
9 endosteal and periosteal surfaces were generated on Avizo v.9. For each vertex of the endosteal
10 surface Avizo computes the distance to the closest point on the periosteal surface. Using this
11 software, the cortical thickness of femoral and tibial shafts can be visualized as a colormap
12 representing the different thickness along the shaft. These colormaps were visually compared in
13 order to discuss the likelihood of an association between two bones.

14 2.2.7. Sex and age-at-death assessments; stature, body mass, and robusticity estimations

15 The sex and age-at-death assessments used in the present study were those published by Gambier et
16 al. (2006) (see this paper for comprehensive descriptions of the methods used). Stature was
17 estimated using Trotter and Gleser (1952, 1958) equation for African-Americans (taking into account
18 remarks from Jantz, et al. (1994)), as suggested by Formicola (2003) for European middle Upper
19 Paleolithic specimens. Body mass was estimated following Ruff, et al. (2018). Robusticity indices
20 were computed from external measurements ($M8 \times 100/M1$ for the femur, and $M10b \times 100/M1$ for
21 the tibia).

22 2.2.8. Comparative samples

23 To characterize specific traits in the Cro-Magnon sample, osteometric values were compared to the
24 Gravettian sample. When this was done, the comparative data never included values for the Cro-
25 Magnon bones and are displayed in the text as "mean \pm one standard deviation (number of
26 individuals considered)". Regression analyses were performed in order to discuss possible
27 associations. These regressions were calculated from an Upper Paleolithic sample, the Gravettian
28 sample alone being too small, once again excluding Cro-Magnon remains. These samples are
29 presented in Villotte et al. (2017), and in the Table 2 of the Supplementary Material 2.

30

31 3. Results and discussion

1 The results are presented by anatomical regions. For each association between two bones presented
2 here, we indicate if it was already mentioned by previous authors (Broca, 1868, Gambier, et al., 2006,
3 Pruner-Bey, 1865–1875, Vallois and Billy, 1965, Villotte, 2009) or, alternatively, if it was explicitly
4 rejected.

5

6 3.1. Pelvis

7 Henry-Gambier et al (2006) identified four individuals, based on four fragments of right coxal bones.
8 However, two of them do not overlap and, in our opinion, belong to the same bone (cf. infra). Thus,
9 three pelvises have been identified, and they will be the core elements for associations, using the sex
10 and age-at-death assessments done by Gambier et al. (2006).

11 The first pelvis is composed by two coxal bones: 4314a and 4314b. The gross morphology is very
12 similar (the two bones appear very “robust”), and both are partly covered by concretions and display
13 significant degenerative changes. The superposition of the left side on the mirrored right side fits
14 perfectly. Thus, their association is almost certain. These two bones were already considered as a
15 pair by Vallois and Billy (1965), Pruner-Bay (1865-1875), and Gambier et al. (2006). As noticed by
16 Gambier et al. (2006), the sacrum 4314c, which was glued to both coxal bones and is still attached to
17 the left one, does not belong to the same individual (see the second pelvis, infra). The pair 4314a and
18 4314b will be the core elements for the individual **Alpha**. This individual is a male (Henry-Gambier et
19 al. 2006), very likely aged considering the degenerative processes present at the joints and entheses
20 (Villotte 2009).

21 The second pelvis is composed of the sacrum 4314c and the fragment of right coxal bone 4316a,
22 likely associated with 4317, and maybe with 4316b. 4316a and 4314c articulate together (Gambier et
23 al. 2006 and SV pers. obs.). Their association is almost certain. They belong to a woman over the age
24 of 60 (Gambier, et al., 2006). 4317 was considered as displaying a female morphology by Pruner-Bey
25 (1865-1875) and Vallois and Billy (1965) but was left unsexed by Henry-Gambier, et al. (2006). 4317
26 and 4316a do not overlap and their gross morphology, size and external appearance point toward
27 two fragments from the same bone, in agreement with Pruner-Bey (1865–1875) and contra Gambier,
28 et al. (2006). The association of these two bones is probable. Their association with the small
29 fragment of ilium 4316b is possible, as the three bones can be virtually replaced on a complete right
30 coxal bone (Fig. 2). The pelvis composed by 4316a, 4314c, 4317 (and possibly 4316b), will form the
31 core element for the individual **Beta**.



1

2 Figure 2. Coxal bone fragments associated with Beta. They are virtually replaced on a complete bone
 3 in order to illustrate their similarities in terms of size and shape.

4

5 The third pelvis is composed of the coxal bones 4318 and 4315, and possibly the sacrum 4319. The
 6 coxal bones have a similar morphology and size, as already noticed by Vallois and Billy (1965) and
 7 Henry-Gambier et al. (2006). The superposition of the left bone on the mirrored right one fits
 8 perfectly. Their association is almost certain. The isolated right sacral auricular surface (4319)
 9 articulates well with the auricular facet of the mirrored 4315. This pelvis is the core element for the
 10 individual **Gamma**, a male aged over 40 years (Henry-Gambier et al. 2006).

11 **3.2. Hip**

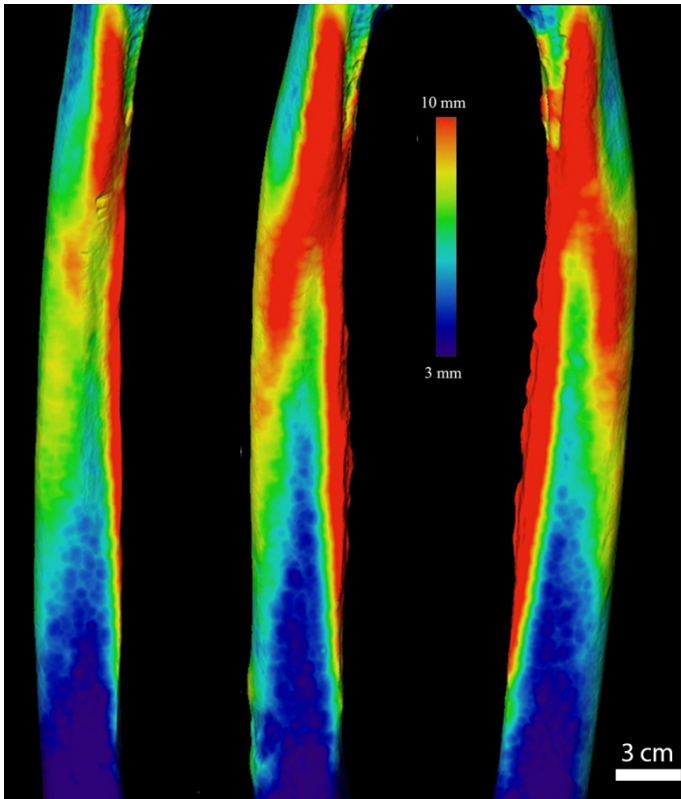
12 Diameters were measured on five acetabula and two femoral heads. The acetabular diameters (AD)
 13 relatively clearly distinguish the three individuals defined from the pelvises (Table 2). The association
 14 of femur 4321 with individuals **Alpha** or **Gamma** is very unlikely. The association of femur 4322 with

1 **Alpha** and **Beta** is very unlikely as well. Based on the relatively clear distinctions between individuals
2 and the good concordance between estimations and real measurements for both FHD and AD, the
3 4321 femur can be associated with **Beta** and the femur 4322 with **Gamma**. Both associations are
4 considered as probable. The association between the right femoral head of 4321 and the right
5 acetabulum of 4317 was already established by Pruner-Bey (1865-1875).

6 3.3. *Thigh*

7 8 femora are identified.

8 The association between 4323/4327 and 4325, two complete diaphyses, is almost certain. They are
9 very similar in term of general morphology (they are both extremely big and robust), size (including
10 their estimated maximum lengths, see Table 3), cortical thickness absolute values and distribution
11 (Fig. 3), degenerative changes (i.e. diffuse cortical irregularity and longitudinal protrusion at fibrous
12 entheses, see Villotte, et al. (2016) for definitions of these terms), surface texture and color. Venous
13 imprints are visible on the cortical surfaces of both bones (Fig. 4). This pair was previously identified
14 by Pruner-Bey (1865-1875), Broca (1868), Vallois and Billy (1965) and Villotte (2009). This pair can be
15 associated with **Alpha** based on the shared surface color (pinkish), degenerative changes at joints
16 and entheses, and the presence on an osteolytic lesion on the external surface of the left iliac blade
17 (near the iliac crest), and a osteolytic lesion (associated with a slight reactive bone production) on the
18 antero lateral part of the distal left diaphysis. This association is almost certain.



1

2 Figure 3. Cortical thickness absolute values and distribution for the most complete femora. From left
 3 to right: 4322, 4325 and 4323 / 4327 (lateral view). Note the great similarities between 4325 and
 4 4323 / 4327.



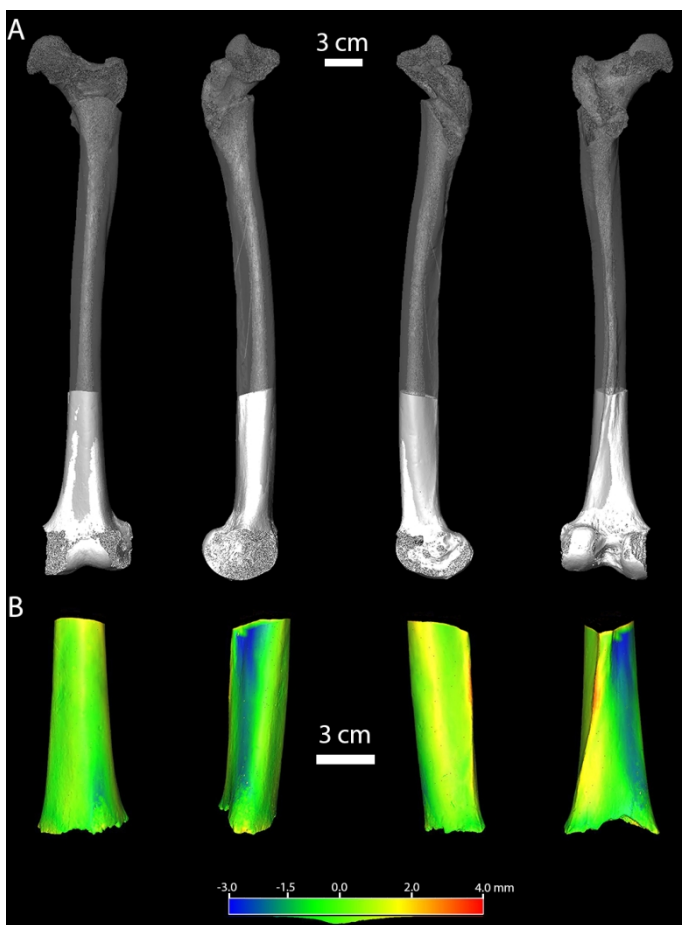
5

6 Figure 4. Venous imprints (black arrows). From left to right: femora 4323 / 4327 and 4325 (medial
 7 views), and tibiae 4331 and 4332 (lateral views).

8

1 4328 and 4322 form another pair. The comparison is harder than for the previous bones, as the
2 overlapping region between these two bones comes down to the distal portion of the shaft (ca. 117
3 mm). However, the general morphology of the inferior end of the linea aspera and the medial and
4 lateral supracondylar ridges is clearly similar (Fig. 5), and the cortical thickness distribution of the
5 region present for the two bones is similar. This association is probable. The analysis of external
6 morphology, size and cortical thickness also allows considering 4323 (a portion of proximal diaphysis)
7 as the probable symmetrical to 4328. Based on results from the hip (cf. 3.2.), the three bones are
8 associated with **Gamma**.

9



10

11 Figure 5. A) Virtual matching of 4322 (grey) and the mirrored model of 4328 (white). B) Distance
12 between the two clouds of points in the overlapping area. From left to right : anterior, medial,
13 lateral, and posterior views.

14

15

1 Three bones are remaining.

2 4329 is a left distal extremity characterized by a small epicondylar breadth (75.0 mm) compared to
3 the shaft. This value is smaller than all the others recorded for the Gravettian adult sample ($84.8 \pm$
4 5.3 (11)). The association of the 4329 is impossible with the left femora 4322 and 4325 and very
5 unlikely with the right femora 4328 (major difference in epicondylar breadth) and 4323 /4327 (major
6 differences in distal shaft morphology and size).

7 4321 (right femoral head and neck) is associated with **Beta**. Its association with 4322, 4323/4327,
8 4325 or 4328 is very unlikely due to the very small size of its articular portion (FHD = 42.2 mm). The
9 correlation between FHD and epicondylar breadth is moderately strong ($R^2 = 0.623$; $N = 29$ Upper
10 Paleolithic individuals; epicondylar breadth = $1.236 * \text{FHD} + 23.976$). Based on this equation, the
11 estimated epicondylar breadth for 4321 would be 76.1 mm, close to the value for 4329. Based on the
12 size of the articular surfaces, especially compared to non articular portions, the association of 4329
13 and 4321, and thus the assignment of 4329 to **Beta**, is considered as probable. This association
14 between these two bones was already proposed by Vallois and Billy (1965).

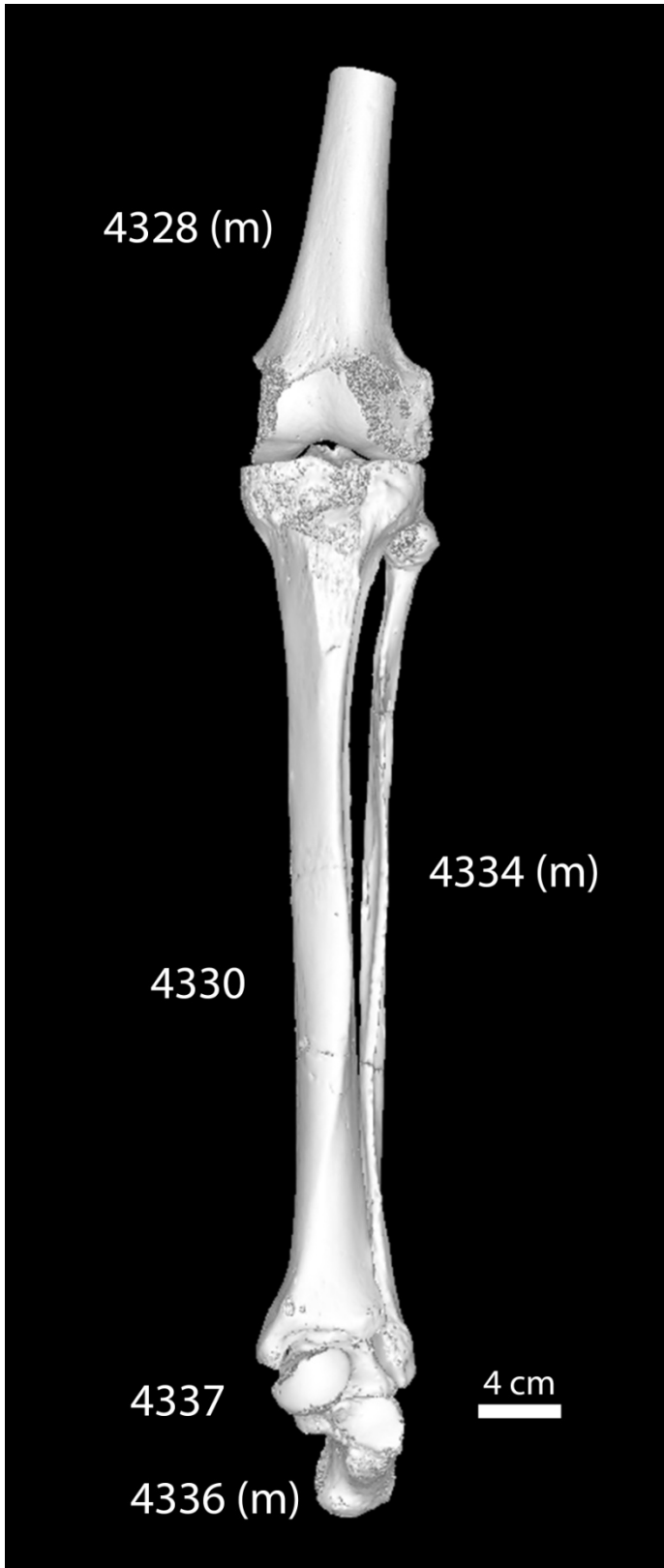
15 4324 is a fragment corresponding roughly to the proximal two-thirds of a left diaphysis. It is not
16 especially robust. Its association with 4322 and 4325 is impossible and seems very unlikely with 4323
17 and 4323/4327. Its association with 4329 (and thus to **Beta**) seems probable, as the two fragments
18 share similar diaphyseal dimensions, and as they are broken roughly at the same location.

19 3.4. *Knee*

20 The femoral distal extremity is preserved for two fragments (4328 and 4329) and the proximal
21 extremity is preserved for one tibia (4330). 4330 and 4329 are both from the left side. Their
22 association is impossible, the distal extremity of the femur 4329 being far too small. The virtual
23 mirroring of 4328 articulates well 4330 (Fig. 6). The medial epicondyle of 4328 is broken but its
24 epicondylar breadth can be estimated to be between 85.0 and 87.0 mm. The value for proximal
25 maximum tibia breadth of 4330 is 78 mm. The correlation between these two measurements is high
26 ($R^2 = 0.868$; $N = 22$ Upper Paleolithic individuals; epicondylar breadth = $1.021 * \text{proximal maximum}$
27 $\text{tibia breadth} + 4.001$). The estimated corresponding epicondylar breadth for 4330 would be 83.3
28 mm, far more than the value for the femur 4329 (75.0 mm) and close to the estimated value for
29 4328. The association of 4328 and 4330, and thus to **Gamma**, was considered as probable.

30

31



1

2 Figure 6. Virtual reconstruction of a lower limb of Gamma. (m): mirrored.

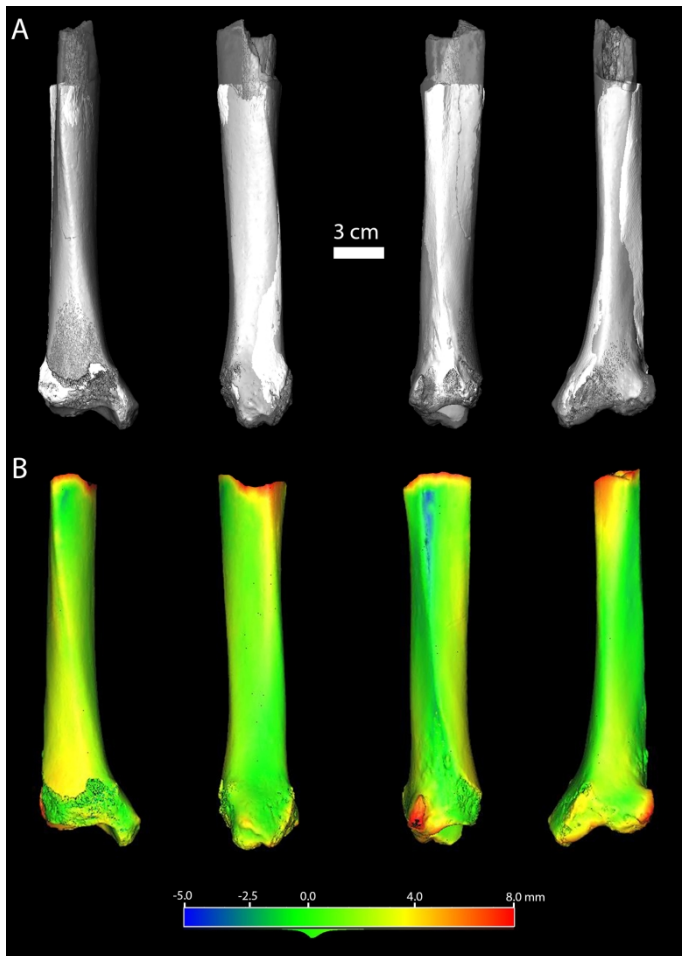
3

4

1 3.5. Leg

2 Four tibial fragments and two fibulae are represented.

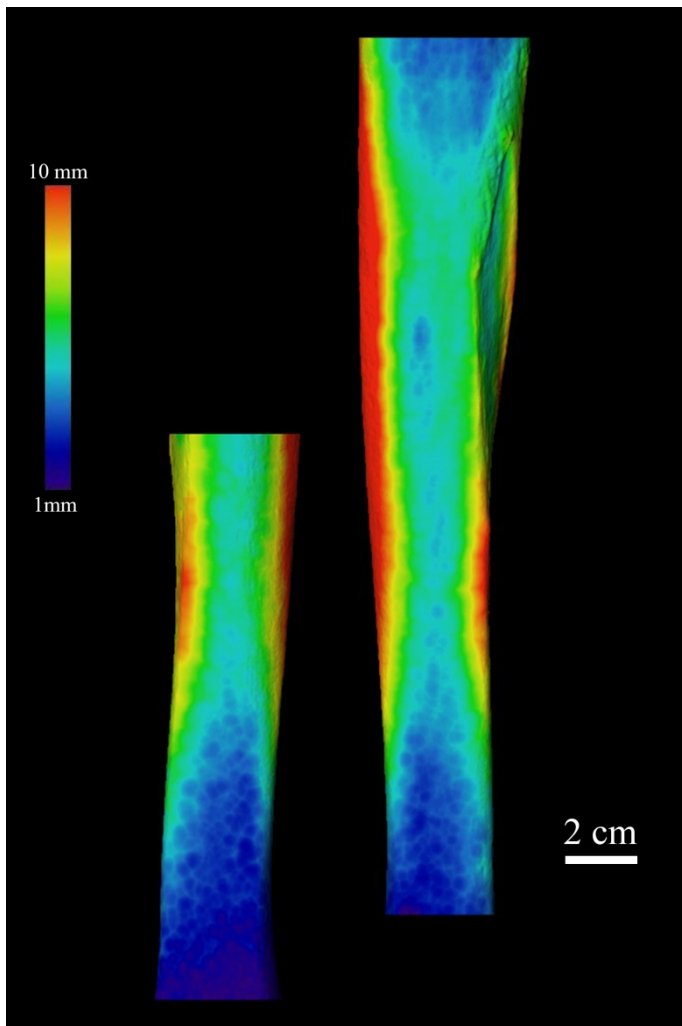
3 The association of the left tibia 4331 and the right tibia 4333 (both represented by the distal half of
4 the bone) is unlikely. The morphology of their distal extremity is quite different, and the mirrored
5 surface rendering of 4331 does not superimpose well on 4333's one, as demonstrated by the
6 considerable distance between the two point clouds in the overlapping area (Fig. 7).



7
8 Figure 7. A) Virtual matching of 4333 (white) and the mirrored model of 4331 (grey). B) Distance
9 between the two clouds of points in the overlapping area. From left to right: anterior, medial, lateral,
10 and posterior views.

11 The association of the left tibia 4331 (distal half) and the right tibia 4332 (diaphysis) is almost certain.
12 They are very similar in term of general morphology and size, their surface models superpose quite
13 well, and their cortical thickness is similar in term of distribution and absolute values (Fig. 8 and 9).
14 Both display venous imprints on the lateral surface of the diaphysis (Fig. 4). Bone production is
15 present in both cases in the area of the tibiofibular syndesmosis. Their surface texture and color are

1 also similar. They share with the femoral pair 4323/4327 and 4325 an impressive robusticity and a
2 great size, a similar color and pathological alterations (degenerative changes and venous imprints).
3 Their association with the femoral pair is thus probable. The right fibula 4335 (proximal half of the
4 diaphysis) can be associated with the tibial pair, based on the very robust aspect of this bone and
5 especially the degenerative changes present at the attachment sites. These three bones can thus be
6 associated with **Alpha**.



7
8 Figure 8. Cortical thickness absolute values and distribution for the left tibia 4331 (distal half) and the
9 right tibia 4332 (diaphysis). Medial views.

10



1

2 Figure 9. A) Virtual matching of 4332 (grey) and the mirrored model of 4331 (white). B) Distance
 3 between the two clouds of points in the overlapping area. From left to right: anterior, medial, lateral,
 4 and posterior views.

5

6 Another almost certain pair is formed by the left tibia 4330 and the right one 4333. Their size and
 7 gross morphology are similar. They share quasi identical squatting facets surrounded superiorly by
 8 vascular foramina, and similar morphology of the medial malleolus (Fig. 10). 4330 articulates well
 9 with the mirrored model of the complete right fibula 4334 (Fig. 6). There is a very strong correlation
 10 between the tibial and fibular maximum lengths ($R^2 = 0.964$; $N = 22$ Upper Paleolithic individuals;
 11 maximum length of the fibula = $0.9661 * \text{maximum length of the tibia} + 5.923$). Based on this
 12 equation, the estimated maximum length of the fibula articulating with 4330 would be 375.0. The

1 estimated maximum length of 4334 is 375.2 mm. The association of 4330 and 4334 is thus almost
2 certain. These three bones belong to **Gamma**.



3
4 Figure 10. Distal view of the tibiae 4333 and 4330.

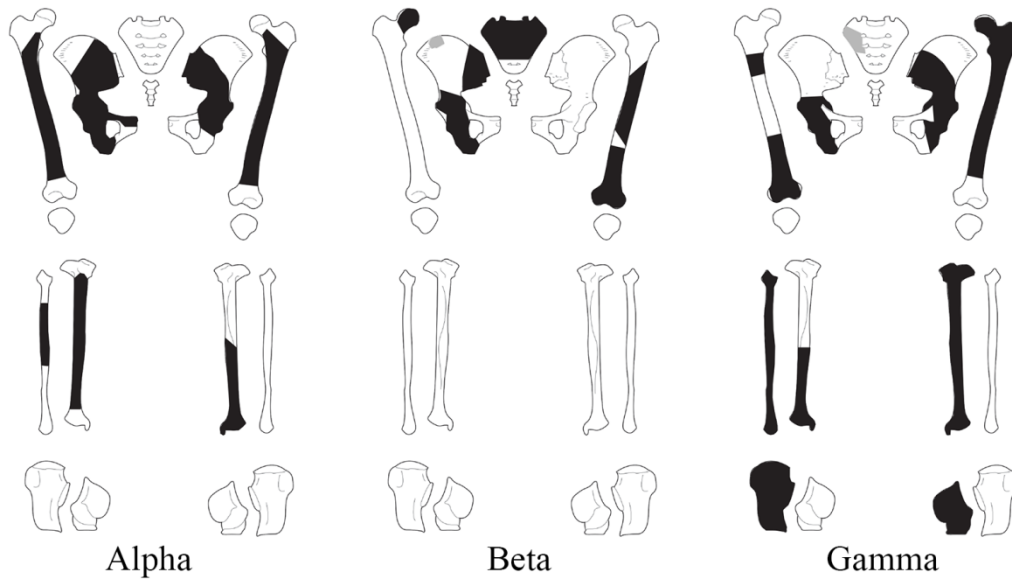
5
6 *3.6. Ankle and foot*

7 Three distal extremities of the tibia and two tali are present. The left talus 4337 is bigger than the
8 right 4338, and they do not share a similar morphology; their association is very unlikely. 4338 does
9 not articulate well with the right tibia 4333, their association is very unlikely as well. Instead, 4338
10 fits relatively well with the mirrored model of the 4331. However, 4338 appears too small to be
11 securely allocated to **Alpha**, and actually its size points more toward an association with **Beta**. 4338
12 was thus not associated with a specific individual. 4337 articulates well with 4330 and with the
13 mirrored model of the fibula 4334 (Fig. 6). Its attribution to **Gamma** is probable. The right calcaneus
14 4336 does not articulate well with 4338 (very unlikely association) but it does with the model of 4337
15 (probable association) (Fig. 6). It was thus allocated to **Gamma**.

16 *3.7. Individual characteristics*

17 In the present study, three individuals have been identified from the lower limb remains (Table 4 and
18 Fig. 11). 25 of 26 bones of lower limbs from Cro-Magnon analyzed here have been associated with
19 one of these individuals.

20



1

2 Figure 11. Skeletal representation of Alpha, Beta and Gamma. In black: probable and almost certain
 3 associations; in grey: possible associations.

Present study	Bone	SV Code	Vallois and Billy (1965)
Alpha	Left coxal bone	4314b	Cro-Magnon 1
	Right coxal bone	4314a	Cro-Magnon 1
	Left femur	4325	Cro-Magnon 1
	Right femur	4323 /4327	Cro-Magnon 1
	Left tibia	4331	Not associated with a specific individual
	Right tibia	4332	Cro-Magnon 1
	Right fibula	4335	Not associated with a specific individual
Beta	Right coxal bone	4317	Cro-Magnon 2
	Right coxal bone	4316a	Not associated with a specific individual
	Right coxal bone	(4316b?)	Not associated with a specific individual
	Sacrum	4314c	Cro-Magnon 1
	Left femur	4324	Not associated with a specific individual
	Left femur	4329	Cro-Magnon 2
	Right femur	4321	Cro-Magnon 2
Gamma	Left coxal bone	4315	Not associated with a specific individual
	Right coxal bone	4318	Not associated with a specific individual
	Sacrum	(4319?)	Not associated with a specific individual
	Left femur	4322	Not associated with a specific individual
	Right femur	4323	Not associated with a specific individual
	Right femur	4328	Cro-Magnon 3
	Left tibia	4330	Cro-Magnon 3
	Right tibia	4333	Cro-Magnon 2
	Right fibula	4334	Cro-Magnon 1
	Left talus	4337	Not associated with a specific individual
	Right calcaneus	4336	Cro-Magnon 1

4

1 Table 4. Associations of bones from Cro-Magnon lower limb remains in the present study and in
2 Vallois and Billy (1965). (XXXX?) indicates that this association is only possible, the other ones being
3 probable or almost certain.

4

5 3.7.1. Individual Alpha

6 Seven bones were allocated to this individual. This adult male is characterized by major pathological
7 changes at joints and entheses likely related to degeneration, indicating an advanced age-at-death.
8 Based on the best preserved bones (i.e. the averaged right and left estimated femoral maximum
9 lengths and the estimated maximum length of the right tibia), his stature can be estimated between
10 170 and 177 cm. His body mass is estimated between 67 and 71 kg (respectively from the right and
11 left FHD). **Alpha** is characterized by high pilastric (left and right averaged = 128.4) and robusticity (left
12 and right averaged = 22.4) indices compared to other Gravettian individuals (respectively 123.0 ± 7.8
13 (19) and 20.3 ± 1.6 (15)), due to extremely developed pilasters and lineae asperae. This impressive
14 development is likely related, at least in part, to degenerative bone production in this area. Individual
15 **Alpha** also has robust tibiae (robusticity index right side = 22.8) compared to the other Gravettian
16 adults (20.6 ± 1.6 (13)). He is also characterized by the presence of focal osteolytic lesions and
17 venous imprints on the cortical surface of the main long bones. Most of the bones are
18 whitish/pinkish and sometimes display concretions on their surfaces. Five bones associated with this
19 individual were assigned to Cro-Magnon 1 by Vallois and Billy in 1965, the last two being not
20 associated with a specific individual by these authors (Table 4). To us, the association with the skull
21 identified as Cro-Magnon 1 is almost certain. First, as noticed previously by many authors (Broca,
22 1868, Gambier, et al., 2006, Pruner-Bey, 1865–1875, Vallois and Billy, 1965, Villotte, 2009), the
23 cranial and lower limb elements share a general external appearance, especially the presence of
24 concretion. Second, the pathological lesions on the frontal and the mandible are of the same nature
25 as those present on the left coxal bone and left femur (Dastugue, 1967, Thillaud, 1985). Thillaud
26 (1985) considered these lesions as part of a syndrome associated to Langerhans cell histiocytosis.
27 Even if, according to Thillaud (1985) himself, this diagnosis is subject to debate, it seems clear that
28 **Alpha** suffered of a systemic, and very likely rare, disease. It is worthwhile noting that rare systemic
29 and difficult to diagnose abnormalities are unusually frequent in the Late Pleistocene sample (see Wu
30 et al. (2013) and Trinkaus et al. (2014) for reviews and discussion).

31 3.7.2. Individual Beta

32 This old woman is characterized by small long bone extremities compared to diaphyses. From the
33 seven fragments of bone allocated to the individual, six are associated with a high degree of

1 confidence and one (the fragment of ilium 4316b) association was considered only as "possible". The
2 stature of **Beta** is estimated between 161 and 167 cm (based on the estimated maximum length of
3 her left femur (i.e. 4324 + 4329)). Her body mass can be estimated to ca. 57 kg. The index of
4 robusticity computed for her left femur (19.2) is below the average for Gravettian sample. Apart the
5 sacrum 4314c incorrectly glued to the coxal bones of Cro-Magnon 1, the bones assigned to this
6 individual were allocated to Cro-Magnon 2 by Vallois and Billy (1965). It could be tempting to
7 associate **Beta** to the cranium labeled as Cro-Magnon 2. However, sexing isolated Upper Paleolithic
8 skulls remains hazardous (Brůžek, et al., 2004, Guyomarc'h, et al., 2017), and the Cro-Magnon 2 skull
9 was classified as undetermined by a linear discriminant analysis based on sexual dimorphic size and
10 shape variables in the Upper Paleolithic sample (Guyomarc'h, et al., 2017). For the moment, it seems
11 more parsimonious to consider **Beta** as an individual solely represented by lower limb remains.

12 3.7.3. Individual Gamma

13 Individual **Gamma** is the most interesting in terms of the new results (Table 4). In the present study,
14 ten bones were allocated to this individual with a high degree of confidence, and one as possible: six
15 of these bones were not associated to a specific individual by Vallois and Billy (1965), two were
16 assigned to Cro-Magnon 1, two were allocated to Cro-Magnon 3, and one was assigned to Cro-
17 Magnon 2. It is worthwhile to notice that **Gamma** is the individual for whom we used most of the
18 different techniques presented in this study to assigned bones. It is an old male, characterized by
19 large long bone extremities compared to the diaphyses. Diffuse cortical irregularity is seen at most
20 fibrous entheses of its femora and tibiae, but rarely associated with longitudinal protrusions. Based
21 on the best preserved bones (left femur and left tibia) his stature can be estimated between 167 and
22 174 cm. His body mass was around 73 kg but it may be overestimated due to the large epiphyses of
23 this individual. His femora and tibiae are less robust than **Alpha** (respectively 19.3 (left femur) and
24 22.5 (right tibia)). There is no argument to preferentially associate **Alpha's** skeletal remains to the
25 cranial remains labeled Cro-Magnon 3 or Cro-Magnon 4 (or even Cro-Magnon 2).

26 3.7.4 Quid of a fourth adult individual?

27 Based on the cranial remains, four adults were identified at Cro-Magnon since the discovery (Broca,
28 1868, Lartet, 1868). However, the allocation of infracranial remains to the cranial individuals was
29 never done in an explicit study. It has been shown here that the two right coxal fragments 4316a and
30 4317, considered by Gambier et al. (2006) as belonging to two different individuals, are actually very
31 likely from the same bone. Thus, based on lower limb skeletal remains, the presence of a fourth adult
32 appears unlikely. Isolated cranial remains are extremely common in Upper Paleolithic sites, even
33 those where more complete skeletons are present (Henry-Gambier and Fauchoux, 2012), and it may

1 the case at Cro-Magnon as well. Further investigations on the upper limb skeletal remains at Cro-
2 Magnon are required in order to test the hypothesis.

3

4 **4. Conclusions**

5 Reassociating bones is extremely time consuming. We must pay tribute to past authors, especially
6 Vallois and Billy (1965) and Gambier et al. (2006), who attempted to identify individuals from the
7 commingled human remains from Cro-Magnon. Our study confirms most of the assignments done
8 previously, at least for two individuals: **Alpha** (i.e. Cro-Magnon 1) and **Beta**. Nevertheless, our study
9 attributed to these two individuals more bones from the lower limbs than was previously done, and
10 more importantly significantly increased and changed the bone assemblage for the third adult called
11 here **Gamma**. This result is in our opinion due to the improvement allowed by virtual analysis of the
12 remains, especially the cortical thickness study and the mirroring, the latter helping greatly for
13 morphological similarities and theoretical articular congruence between two bones from different
14 sides. This study will be pushed further with the analysis of the upper limbs remains with similar
15 techniques and with independent macroscopic analyses done by other experimented anatomists.
16 Further analyses will also allow us to discuss the presence of upper limb remains of a fourth adult,
17 which was not identified nor even suspected in our study of the lower limb skeletal assemblage. We
18 hope that a comprehensive study, including the analyses for the upper limb remains but also the
19 descriptions of the state of preservation and the anatomical features of each bone, and the
20 osteometric and non-metric data, will significantly improve our knowledge of the people from Cro-
21 Magnon and more broadly from the Late Pleistocene.

22

23 **Fundings**

24 This work was supported by the Agence National de la Recherche (ANR) (Gravett'Os Project; Principal
25 investigator: SV; grant number: ANR-15-CE33-0004). The funding source had no involvement in the
26 study design, the collection, analysis and interpretation of data, nor in the decision to submit this
27 article for publication.

28

29 **Acknowledgements**

1 SV thanks Veronique Laborde, Aurélie Fort (curators of the Musée de L'Homme) and Dominique
2 Grimaud-Hervé (in charge of the collection) for granting the access to the human remains. SV
3 especially thanks Veronique Laborde for the great amount of work done in order to prepare the
4 bones for the micro-CT data acquisition. SV is grateful to Dominique Henry-Gambier for sharing her
5 knowledge about Cro-Magnon site and human remains and for giving him the initial database of the
6 human remains. AT thanks Patricia Wils (MNHN) for is help with the micro-CT data. The authors
7 thank Ronan Ledevin (PACEA), Frédéric Santos (PACEA) and Pierre Guyomarc'h (PACEA and
8 International Committee of the Red Cross) for useful discussions about the data acquired. The 3D
9 surface models used to estimate the maximal length of the bones were kindly provided by Vitale
10 Sparacello (PACEA). Thanks to him for this and for his advices to AT on the estimation procedure. AT
11 thanks Bruno Dutailly (PACEA and Archéovision) for providing advices on TIVMI. The osteometric
12 data used to compare Cro-Magnon individuals were mostly collected by SV (from actual bones or
13 from the literature) but also kindly provided by Trenton Holliday (Tulane University), Mathilde Samsel
14 (PACEA), Vitale Sparacello (PACEA), and Erik Trinkaus (Washington University). SV is grateful to all of
15 them. The authors thank Erik Trinkaus, the two anonymous reviewers and the editor for their useful
16 comments on the first version of this article.

17

18 **Footnotes**

19 1. It should be noted that many bone samples have been taken from Cro-Magnon skeletal remains in
20 order to obtain ancient DNA or collagen for C14 dating. None of the analyses has provided results
21 (Henry-Gambier, et al., 2013a), apart from a bone that clearly does not come from the site of Cro-
22 Magnon (see footnote 2).

23 2. Two femoral shafts (25 290 and 25 291) curated with the other remains, clearly do not come from
24 the site of Cro-Magnon (see Henry-Gambier et al. (2013a) for detailed arguments to exclude them
25 from this sample). They are thus not included in this database. One of them has been dated to $690 \pm$
26 39 BP by Fu et al. (2013). This date and the mitochondrial genome from this femur were published
27 with the misleading label "Cro-Magnon 1".

28

29 **References cited**

30 Auerbach, B.M., Ruff, C.B., 2006. Limb bone bilateral asymmetry: variability and commonality among
31 modern humans, *J. Hum. Evol.* 50, 203-218.

1 Bräuer, G., 1988. Osteometrie, in: Knussmann, R. (Ed.), *Anthropologie: handbuch der vergleichenden*
2 *Biologie des Menschen*, G. Fischer, Stuttgart, pp. 160-232.

3 Broca, P., 1868. Sur les crânes et ossements des Eyzies, *Bulletins de la Société d'Anthropologie de*
4 *Paris 2e série*, 3, 350-392.

5 Brůžek, J., Schmitt, A., Murail, P., 2005. Identification biologique individuelle en paléanthropologie.
6 Détermination du sexe et estimation de l'âge au décès à partir du squelette, *Objets et méthodes en*
7 *paléanthropologie*, 217-246.

8 Brůžek, J., Šefčáková, A., Černý, V., 2004. Révision du sexe des squelettes épipaléolithiques de
9 Taforalt et d'Afalou-bou-Rhoummel par une approche probabiliste, *Antropo* 7, 195-202.

10 Coleman, M.N., Colbert, M.W., 2007. Technical note: CT thresholding protocols for taking
11 measurements on three-dimensional models, *Am. J. Phys. Anthropol.* 133, 723-725.

12 Dastugue, J., 1967. Pathologie des hommes fossiles de l'abri de Cro-Magnon, *L'Anthropologie* 71,
13 479-492.

14 Finnegan, M., 1978. Non-metric variation of the infracranial skeleton, *J. Anat.* 125, 23-37.

15 Formicola, V., 2003. More is not always better: Trotter and Gleser's equations and stature estimates
16 of Upper Paleolithic European samples, *J. Hum. Evol.* 45, 239-244.

17 Fu, Q., Mittnik, A., Johnson, Philip L.F., Bos, K., Lari, M., Bollongino, R., Sun, C., Giemisch, L., Schmitz,
18 R., Burger, J., Ronchitelli, Anna M., Martini, F., Cremonesi, Renata G., Svoboda, J., Bauer, P.,
19 Caramelli, D., Castellano, S., Reich, D., Pääbo, S., Krause, J., 2013. A Revised Timescale for Human
20 Evolution Based on Ancient Mitochondrial Genomes, *Curr. Biol.* 23, 553-559.

21 Gambier, D., 1986. Etude des os d'enfants du gisement aurignacien de Cro-Magnon, Les Eyzies
22 (Dordogne), *Bulletins et Mémoires de la Société d'Anthropologie de Paris* 3, 13-25.

23 Gambier, D., Bruzek, J., Schmitt, A., Houët, F., Murail, P., 2006. Révision du sexe et de l'âge au décès
24 des fossiles de Cro-Magnon (Dordogne, France) à partir de l'os coxal, *C. R. Palevol* 5, 735-741.

25 Guyomarc'h, P., Samsel, M., Courtaud, P., Mora, P., Dutailly, B., Villotte, S., 2017. New data on the
26 paleobiology of the Gravettian individual L2A from Cussac cave (Dordogne, France) through a virtual
27 approach, *Journal of Archaeological Science: Reports* 14, 365-373.

28 Henry-Gambier, D., 2002. Les fossiles de Cro-Magnon (Les eyzies-de-Tayac, Dordogne) : nouvelles
29 données sur leur position chronologique et leur attribution culturelle, *Bulletins et Mémoires de la*
30 *Société d'Anthropologie de Paris n.s.*, 14, 89-112.

31 Henry-Gambier, D., 2008a. Comportement des populations d'Europe au Gravettien : Pratiques
32 funéraires et interprétations, *Paleo* 20, 399-438.

33 Henry-Gambier, D., 2008b. Les sujets juvéniles du Paléolithique supérieur d'Europe à travers
34 l'analyse des sépultures primaires : L'exemple de la culture gravettienne, in: F. Gusi, Olaria, D.C.,
35 Muriel, L.S. (Eds.), *La muerte en la infancia*, Servicio de Investigaciones Arqueológicas y Prehistoricas
36 de la Diputacion de Castellon y el Laboratorio de Arqueologia Prehistorica de la Universidad « Jaume
37 1 » de Castellon, Castelló, pp. 331-364.

38 Henry-Gambier, D., Fauchoux, A., 2012. Les pratiques autour de la tête en Europe au Paléolithique
39 supérieur, in: Boulestin, B., Henry-Gambier, D. (Eds.), *Crânes trophées, crânes d'ancêtres et autres*
40 *pratiques autour de la tête : problèmes d'interprétation en archéologie*, BAR, Oxford, pp. 53-67.

41 Henry-Gambier, D., Nespoulet, R., Chiotti, L., 2013a. An Early Gravettian cultural attribution for the
42 human fossils from the Cro-Magnon rock shelter (Les Eyzies-de-Tayac, Dordogne), *Paleo* 24, 121-138.

43 Henry-Gambier, D., Villotte, S., Beauval, C., Brůžek, J., Grimaud-Hervé, D., 2013b. Les vestiges
44 humains : un assemblage original, in: Nespoulet, R., Chiotti, L., Henry-Gambier, D. (Eds.), *Le*
45 *Gravettien final de l'abri Pataud (Dordogne, France). Fouilles et études 2005-2009*, Archaeopress,
46 BAR International Series, 2458, Oxford, pp. 135-177.

47 Jantz, R.L., Hunt, D.R., Meadows, L., 1994. Maximum length of the tibia: How did Trotter measure it?,
48 *Am. J. Phys. Anthropol.* 93, 525-528.

49 Knüsel, C.J., Outram, A., 2004. Fragmentation: The Zonation Method Applied to Fragmented Human
50 Remains from Archaeological and Forensic Contexts, *Environmental Archaeology* 9, 85-98.

51 Lartet, L., 1868. Une sépulture des troglodytes du Périgord, *Bulletins de la Société d'Anthropologie*
52 *de Paris* 3, 335-349.

1 Murail, P., Bruzek, J., Houët, F., Cunha, E., 2005. DSP: a tool for probabilistic sex diagnosis using
2 worldwide variability in hip-bone measurements *Bulletins et Mémoires de la Société d'Anthropologie*
3 *de Paris n.s.*, 17, 167-176.

4 Plavcan, J.M., Hammond, A.S., Ward, C.V., 2014. Brief Communication: Calculating hominin and
5 nonhuman anthropoid femoral head diameter from acetabular size, *Am. J. Phys. Anthropol.* 155, 469-
6 475.

7 Pruner-Bey, F., 1865-1875. An account of the human bones found in the cave of Cro-Magnon in
8 Dordogne, in: Lartet, E., Christy, H. (Eds.), *Reliquiae Aquitanicae: being Contributions to Anthropology*
9 *and Palaeontology of Périgord and the Adjoining Provinces of Southern France*, vol. 1, William and
10 Morgate, London, pp. 73-92.

11 Ruff, C.B., Burgess, M.L., Squyres, N., Junno, J.-A., Trinkaus, E., 2018. Lower limb articular scaling and
12 body mass estimation in Pliocene and Pleistocene hominins, *J. Hum. Evol.* 115, 85-111.

13 Schindelin, J., Arganda-Carreras, I., Frise, E., Kaynig, V., Longair, M., Pietzsch, T., Preibisch, S., Rueden,
14 C., Saalfeld, S., Schmid, B., Tinevez, J.-Y., White, D.J., Hartenstein, V., Eliceiri, K., Tomancak, P.,
15 Cardona, A., 2012. Fiji: an open-source platform for biological-image analysis, *Nat. Meth.* 9, 676.

16 Sládek, V., Trinkaus, E., Hillson, S.W., Holliday, T.W., 2000. The people of the Pavlovian. Skeletal
17 catalogue and osteometrics of the Gravettian fossil hominids from Dolní Věstonice and Pavlov,
18 Academy of Sciences of the Czech Republic, Brno.

19 Sparacello, V.S., Villotte, S., Shackelford, L.L., Trinkaus, E., 2017. Patterns of Humeral Asymmetry
20 among Late Pleistocene Humans, *Comptes Rendus Palevol.* 16, 680-689.

21 Spoor, C.F., Zonneveld, F.W., Macho, G.A., 1993. Linear measurements of cortical bone and dental
22 enamel by computed tomography: Applications and problems, *Am. J. Phys. Anthropol.* 91, 469-484.

23 Thillaud, P.L., 1985. L'homme de Cro-Magnon et ses maladies, *Les dossiers d'archéologie* 97, 67-73.

24 Trinkaus, E., Buzhilova, A.P., Mednikova, M.B., Dobrovolskaya, M.V., 2014. *The People of Sunghir.*
25 *Burials, Bodies, and Behavior in the Earlier Upper Paleolithic*, Oxford University Press, New York.

26 Trotter, M., Gleser, G.C., 1952. Estimation of stature from long limb bones of American Whites and
27 Negroes *Am. J. Phys. Anthropol.* 10, 463-514.

28 Trotter, M., Gleser, G.C., 1958. A re-evaluation of estimation of stature based on measurements of
29 stature taken during life and of long bones after death, *Am. J. Phys. Anthropol.* 16, 79-123.

30 Vallois, H.V., Billy, G., 1965. Nouvelles recherches sur les hommes fossiles de l'abri de Cro-Magnon,
31 *L'Anthropologie* 69, 47-74.

32 Villotte, S., 2009. *Enthésopathies et activités des Hommes préhistoriques - Recherche*
33 *méthodologique et application aux fossiles européens du Paléolithique supérieur et du Mésolithique*,
34 *Archaeopress*, Oxford.

35 Villotte, S., Assis, S., Cardoso, F.A., Henderson, C.Y., Mariotti, V., Milella, M., Pany-Kucera, D., Speith,
36 N., Wilczak, C.A., Jurmain, R., 2016. In search of consensus: Terminology for enthesal changes (EC),
37 *International Journal of Paleopathology* 13, 49-55.

38 Villotte, S., Samsel, M., Sparacello, V., 2017. The paleobiology of two adult skeletons from Baouso
39 da Torre (Bausu da Ture) (Liguria, Italy): Implications for Gravettian lifestyle, *Comptes Rendus Palevol*
40 16, 462-473.

41 Wright, L.E., Vásquez, M.A., 2003. Estimating the length of incomplete long bones: Forensic
42 standards from Guatemala, *Am. J. Phys. Anthropol.* 120, 233-251.

43 Wu, X.-J., Xing, S., Trinkaus, E., 2013. An enlarged parietal foramen in the late archaic Xujiayao 11
44 neurocranium from Northern China, and rare anomalies among Pleistocene *Homo*, *PLoS ONE* 8,
45 e59587.

Supplementary information 1. Pictures of the 26 bones under study in "Disentangling Cro-Magnon: a multiproxy approach to reassociate lower limb skeletal remains and to determine the biological profiles of the adult individuals."

Authors: Adrien Thibeault, Sébastien Villotte

All the pictures were done by S. Villotte. Scales: White bar = 5 cm.

Left coxal bone 4314a



Right coxal bone 4314b and sacrum 4314c



Left coxal bone 4315



Right coxal bone 4316a



Right coxal bone 4316b



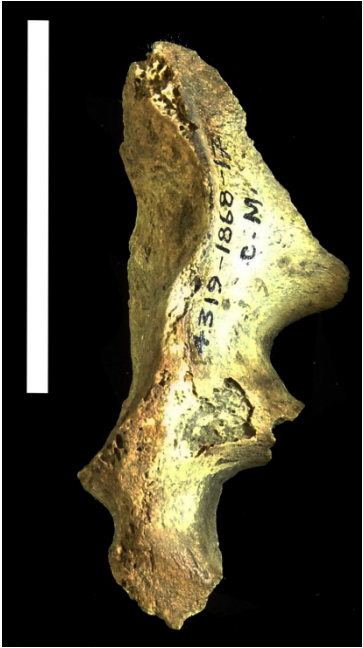
Right coxal bone 4317



Right coxal bone 4318



Sacrum 4319



Right femur 4321



Right femur 4323



Right femur 4328



Right femur 4323 / 4327



Left femur 4324



Left femur 4325



Left femur 4329



Left femur 4322



Right tibia 4333



Right tibia 4332



Left tibia 4331



Left tibia 4330



Right fibula 4334



Right fibula 4335



Right talus 4338



Left talus 4337



Right calcaneus 4336



Supplementary information 2. "Disentangling Cro-Magnon: a multiproxy approach to reassociate lower limb skeletal remains and to determine the biological profiles of the adult individuals."

Authors: Adrien Thibeault, Sébastien Villotte

Table 1. Upper Paleolithic skeletons used for estimation of bone maximal dimensions from virtual models. L = Left; R = Right

Bone	Individuals
Femur	Barma Grande 2 (L), Arene Candide 2 (R), Arene Candide 4 (R), Arene Candide 12 (R), San Teodoro 1 (L)
Tibia	Barma Grande 2 (L), Barma Grande 5 (R), Arene Candide 2 (R), Arene Candide 4 (L), Arene Candide 10 (L)
Fibula	Barma Grande 2 (L), Barma Grande 5 (R), Arene Candide 4 (R and L), Arene Candide 12 (R)

Table 2. European Middle and Late Upper Paleolithic comparative sample.

Period	Males	Females	Uncertain sex
Middle Upper Paleolithic (i.e. Gravettian s. l.)	Barma Grande 2, 5, 6; Dolní Věstonice 13, 14, 16; Grotte-des-Enfants 4; Parabita 1; Pataud 5; Paviland 1; Pavlov 1; Sunghir 1.	Caviglione 1; Dolní Věstonice 3; Grotte-des-Enfants 5; Ostuni 1; Paglicci 25; Parabita 2; Pataud 3.	Dolní Věstonice 35; Předmostí 1, 3, 4, 9, 10, 14; Sunghir 4.
Late Upper Paleolithic	Arene Candide 2, 3, 4, 5, 10, 12; Bichon; Continenza 7; Laugerie Basse 4; Los Azules; Oberkassel 1; Peyrat 5; Riparo Tagliente; Rochereil; Romanelli 1; Romito 3, 4; Villabruna 1.	Cap Blanc 1; Cova Fosca A 1 AD; Grotte-des-Enfants 3; Lafaye 1; Oberkassel 2; Romito 1, 5, 6; San Teodoro 1, 4; St-Germain-la-R. 4.	Arene Candide 14; Chancelade 1; Farincourt 1; Les Forges E546; Madeleine 1; Maritza 2; Placard 16; Romanelli 4.